Published in final edited form as:
Bone. 2015 April ; 0: 90–97. doi:10.1016/j.bone.2014.12.014.

A phase I feasibility study of multi-modality imaging assessing rapid expansion of marrow fat and decreased bone mineral density in cancer patients

Susanta K Hui[1,2], **Luke Arentsen**[1], **Thanasak Sueblinvong**[3], **Keenan Brown**[4], **Pat Bolan**[5], **Rahel G Ghebre**[3], **Levi Downs**[3], **Ryan Shanley**[6], **Karen E. Hansen**[7], **Anne G. Minenko**[8], **Yutaka Takhashi**[2], **Masashi Yagi**[2,9], **Yan Zhang**[6], **Melissa Geller**[3], **Margaret Reynolds**[1], **Chung K Lee**[1], **Anne H. Blaes**[2,8], **Sharon Allen**[10], **Bruno Beomonte Zobel**[11], **Chap Le**[12], **Jerry Froelich**[5], **Clifford Rosen**[13], and **Douglas Yee**[2,8]

[1]Department of Therapeutic Radiology, Austin TX, USA

[2]Masonic Cancer Center, Austin TX, USA

[3]Department of Obstetrics and Gynecology, Austin TX, USA

[4]Mindways Software Inc., Austin TX, USA

[5]Center for Magnetic Resonance Research, Department of Radiology, University of Wisconsin, Madison, USA

[6]Biostatistics Core, Masonic Cancer Center, University of Wisconsin, Madison, USA

[7]Department of Medicine, Division of Rheumatology, University of Wisconsin, Madison, USA

[8]Department of Medicine, Osaka, Japan

[9]Osaka University, Osaka, Japan

[10]Family Medicine and Community Health, School of Medicine, Rome, Italy

[11]Campus Bio-Medico University, School of Medicine, Rome, Italy

[12]Department of Biostatistics, University of Minnesota, Minneapolis

[13]Maine Medical Center Research Institute, Scarborough, Maine, USA

Abstract

Address for correspondence: Susanta K Hui, PhD, Department of Therapeutic Radiology, University of Minnesota, 420 Delaware Street SE, Mayo Mail Code 494, Minneapolis, MN 55455, Phone: 612-626-4484, Fax: 612-626-7060; huixx019@umn.edu.

Disclosures: KB is a stockholder and employee of Mindways Software.

Authors' roles: Study design: SH, DY, AM, LD, PB, RG, JF, CL, YZ. Study conduct and data collection: LA, SH, TS, PB, RG, MG, MR, YT, MY, LD. Data analysis: SH, LA, RS, YZ, KB, KH. Data interpretation: SH, DY, CR, KH, KB, BZ, AB, RS. Drafting manuscript: SH, DY, KH, CR, KB, PB, RS.

Purpose—Cancer survivors are at an increased risk for fractures, but lack of effective and economical biomarkers limits quantitative assessments of marrow fat (MF), bone mineral density (BMD) and their relation in response to cytotoxic cancer treatment. We report dual energy CT (DECT) imaging, commonly used for cancer diagnosis, treatment and surveillance, as a novel biomarker of MF and BMD.

Methods—We validated DECT in pre-clinical and Phase I clinical trials and verified with water-fat MRI (WF-MRI), quantitative CT (QCT) and dual-energy X-ray absorptiometry (DXA). Basis material composition framework was validated using water and small-chain alcohols simulating different components of bone marrow. Histologic validation was achieved by measuring percent adipocyte in cadaver vertebrae and compared with DECT and WF-MRI. For a Phase I trial, sixteen patients with gynecologic malignancies (treated with oophorectomy, radiotherapy or chemotherapy) underwent DECT, QCT, WF-MRI and DXA before and 12 months after treatment. BMD and MF percent and distribution were quantified in lumbar vertebrae and the right femoral neck.

Results—Measured precision (3 mg/cm^3) was sufficient to distinguish test solutions. Adiposity in cadaver bone histology was highly correlated with MF measured using DECT and WF-MRI ($r = 0.80$ and 0.77, respectively). In the clinical trial, DECT showed high overall correlation ($r = 0.77$, 95% CI: 0.69, 0.83) with WF-MRI. MF increased significantly after treatment ($p<0.002$). Chemotherapy and radiation caused greater increases in MF than oophorectomy ($p<0.032$). L4 BMD decreased 14% by DECT, 20% by QCT, but only by 5% by DXA ($p<0.002$ for all). At baseline, we observed a statistically significant inverse association between MF and BMD which was dramatically attenuated after treatment.

Conclusion—Our study demonstrated that DECT, similar to WF-MRI, can accurately measure marrow adiposity. Both imaging modalities show rapid increase in MF following cancer treatment. Our results suggest that MF and BMD cannot be used interchangeably to monitor skeletal health following cancer therapy.

Keywords

Dual energy CT; water-fat MRI; Quantification; visualization of bone marrow

INTRODUCTION

Cancer survivors experience a greater risk of fracture compared to the general population (1–6). However, the effect of cancer treatment, especially the relationship between marrow fat (MF) and bone mineral density (BMD), are not well known. Mesenchymal stem cells (MSC) are non-hematopoietic, pluripotent marrow progenitor cells which give rise primarily to osteoblasts and adipocytes. Bone and marrow (B&M) represent a functional biological entity, with evidence of bi-directional co-regulation of bone and marrow components (7,8). Under the influence of radiotherapy or chemotherapy, MSCs demonstrate enhanced commitment to adipogenesis (9,10), resulting in reduced osteogenic potential (11) and increased MF, one source of circulating adiponectin (12). Bone marrow fat was associated with vertebral fracture in older adults and postmenopausal women (13). The rapid increase in marrow fat after cytotoxic cancer therapy in pre-clinical studies (14,15) and a recent

retrospective clinical study revealing post treatment early fracture events (16) emphasizes the need to assess MF along with bone in cancer patients. However, changes in MF are not readily detected by a traditional dual-energy X-ray absorptiometry (DXA) scan, since DXA only calculates average BMD by superimposing cortical and cancellous BMD. Indeed, we demonstrated that radiation-induced increases in MF were not reflected in equivalent loss of cancellous bone in ovariectomized compared with intact mice (14).

Increased MF could also affect the BMD since the physical density of fat/yellow marrow (YM) and red marrow (RM) are different (17,18). The BMD could be lower by up to 10.8 mg/cc in the presence of 10% marrow fat. The apparent BMD of red marrow is approximately 50 mg/cm^3 higher than the BMD of yellow marrow (19,20). Since cancellous bone is composed mostly of marrow (70% at the age of 25) (21), change in marrow composition may confound true change in trabecular bone density if they are not distinguished. Dual energy CT (DECT) uses differential attenuation from two energies for marrow correction (22), but has never been translated into osteoporosis clinical care. This may be due to the high radiation dose exposure from multiple CT scans using older scanners, or because age-related osteoporosis typically results in only modest changes in marrow composition. In contrast, cancer treatment induces large changes in marrow composition (23–25). Moreover, water-fat MRI (WF-MRI) could also measure volumetric marrow composition (26). However, MRI use is limited in cancer patients after diagnosis, perhaps due to its high cost. Furthermore, MRI alone cannot accurately measure bone mineral density and therefore assess risk. In contrast, CT scan is part of routine cancer diagnosis, radiotherapy treatment planning and disease surveillance. DECT could provide multiple time points of measurement without requiring additional CT scans and the additional cost or radiation burden. Furthermore newly developed iterative reconstruction technology has significantly reduced the radiation dose to patients and improved imaging quality of DECT (27). Thus DECT is economically viable and advantageous. However, DECT has never been used to measure marrow fat and it is also unknown if the DECT-predicted MF will be equivalent to MF measured using WF-MRI. In this trial, we hypothesized that DECT and WF-MRI could reliably measure changes in MF associated with cancer treatments.

The ultimate goal is to develop clinically useful biomarkers to predict, measure, and monitor cancer-therapy induced bone loss, thereby individualizing therapy to decrease bone morbidity and ultimately enhancing quality of life for cancer survivors. The aims of this pilot translational study consisted of two-steps: reporting pre-clinical validation of DECT predicting MF simulating in physical space with basis material composition and correlating imaging modalities with histology in cadavers. With these results, a clinical feasibility study was conducted with Aim 1) to assess the possibility of DECT as a biomarker to quantify the effects of cancer treatments on MF by comparing with the simultaneously measured and previously established WF-MRI method. Secondary aims of this study were to assess effects of cancer treatment modalities (oophorectomy, chemotherapy and radiation) on MF expansion and mapping of MF distribution, and Aim 2) to test if commonly known inverse correlations between MF and BMD holds true in patients undergoing cancer treatment (14). Secondary aim was to measure sensitivity of BMD comparing DECT, QCT and DXA.

METHODS

Pre-clinical validation of DECT

Somatom Definition Flash (Siemens, Germany) is used for DECT (at 140 and 80kVp) scan and 80kVp energy in single energy or QCT scan. For pre-clinical validation of DECT, basis material composition estimates for bone regions were derived relative to the manufacturer-reported basis material compositions for the CT calibration phantom. XCOM, an X-ray attenuation database, was used to estimate basis material compositions calculations for the following series of five compounds: water, methanol (50%), ethanol (95%), 2-propanol (70%) and 1-butanol (100%) (28,29). Basis material compositions were also estimated for yellow marrow and red marrow using average atomic compositions from International Commission on Radiation Units & Measurements (ICRU)-46 report in XCOM for these marrow types with assumed physical densities of 0.93 g/cm^3 and 1.03 g/cm^3, respectively (30). Basis material density estimates were observed to have a precision on the order of 3 mg/cm^3. Measurement precision was sufficient to distinguish the series of test solutions in the two dimensional basis material spaces. More details are in the supplement section.

Pre-clinical correlation between DECT and WF-MRI

Detailed methodology of physiological verification is communicated separately (31). Briefly, five female donors (mean age of 56.8 ± 8.2 years) were scanned by DECT (1mm slice thickness at 140 and 80kVp energy in single scan) and WF-MRI (3 Tesla MRI scanner, Tim TRIO, Siemens Medical Solutions, Malvern, PA, USA) imaging sequentially, within 24 hours postmortem. Seventeen lumber vertebrae samples were then removed, decalcified, paraffin embedded, and stained with hematoxylin and eosin (H&E). The ratio of adipocyte volume per tissue volume (AV/TV) was extracted from the histology sample and a correlation between DECT and WF-MRI MF calculation was obtained. Taking a histologic section from the center of the vertebral body ensured that the AV/TV was taken from a representative section of the imaging ROI. In order to test intra-sample variability, histologic examinations were also performed at 0.5cm superior and 0.5cm inferior to the middle in three vertebral bodies and the average coefficient of variation between the sections was found to be 0.08. Inter-user variability between the two users as seen by an intraclass correlation coefficient of $r = 0.984$.

Clinical feasibility trial

Women >18 years old with newly diagnosed ovarian and endometrial cancer who planned to receive chemotherapy or radiation therapy following oophorectomy were considered eligible for the study. We excluded women with osteoporosis, hyperparathyroidism and those who had received chemotherapy, radiation or hormonal therapy within the prior year. The study was approved by the University of Minnesota Institutional Review Board and subjects provided written consent. Thirty one patients were recruited for this study.

Twelve women with early stage ovarian or endometrial cancer who underwent surgical oophorectomy but not adjuvant chemotherapy or radiation therapy served as the control group.

Ovarian cancer patients (n=13) were treated with carboplatin and paclitaxel 175 mg/m^2 every 21 days for ≥6 cycles. Endometrial cancer patients (n=6) were primarily treated using external beam radiation therapy (EBRT) to the pelvis (median dose, 45–50 cGy in 25–28 fractions) and additional radiation at the vaginal surface using high dose rate (HDR) brachytherapy. The radiation window encompassed the pelvis up to ~L5. Though radiation fields covered up to L5 with a dose of 45 Gy, L4 and L3 fell in a dose gradient region. Thus, to include the radiation dose gradient, we chose to include the L3–L5 spine for this study.

DECT (at 140 and 80kVp energy in single scan) scanning (Somatom Definition Flash, Siemens, Germany) was performed on 31 patients at baseline, 6 and 12 months after treatment. A CT calibration phantom (Mindways Software, Austin, TX), commonly used for bone densitometry, was positioned under each patient and spanned the scanned volume which extended from L3 through the right femoral neck. QCT Pro (Mindways Software, Austin, TX) was used to derive single-energy (140 kVp) volumetric BMD estimates. DXA (GE Healthcare Lunar Prodigy, Madison, WI) was also performed at 0 and 12 months. To validate DECT as a imaging biomarker, to measure treatment induced change in MF, simultaneous to DECT imaging, 16 patients also unerwent WF-MRI scans at 0, 6 and 12 months using a 3 T Siemens TRIO scanner (TIM Trio, Siemens, Erlangen, Germany). Images were obtained at L3–L5 and the right femoral neck (FN). Detail on the WF-MRI method is given elsewhere (32). Briefly, three consecutive 3D images were acquired with TR=9 ms, TE=2, 3, and 4 ms, parallel imaging acceleration 3×2 and nominal resolution of 1.1 × 1.1 × 2.45 mm. The WF reconstruction was performed using the method of Berglund et al. (20). The 3D fat fraction image was calculated as MF = fat/(fat+water) and exported in DICOM format for analysis.

Patient measurements were projected onto the line in the basis material space connecting the basis material composition of yellow marrow and that of water using a minimum distance projection, P, parameterized such that the position P=100% corresponded to yellow marrow and the position P=0% corresponded to water. We performed linear transformation of the DECT fat-fraction estimates to the MRI fat-fraction scale, taking into account average BMD among the study subjects. The CT-derived estimate of MF was calculated using: MF = 0.348 * P + 85.7%. The transformation did not impact measurement correlation, supporting its use in detection of longitudinal changes in fat fraction.

Statistical analysis

Statistical models were used to evaluate BMD and MF trends over time by treatment, skeletal region, and imaging modality. Graphical methods such as scatterplots and boxplots identified important relationships, such as measurement distributions and within-patient correlation over time, which informed analysis methods. Linear regression was used to estimate the functional relationship between DECT and WF-MRI MF measurements. Differences in MF or BMD based on treatment or skeletal region were analyzed using generalized estimating equations (GEE*) models (33), with each model employing one outcome measured by a single imaging modality. Each model had main effects for age, time (0, 6 and 12 months) and treatment (or region), an interaction effect of time and treatment (or region) and modeled within-subject correlation using an exchangeable structure.

Wilcoxon signed rank tests were applied to evaluate changes over time for individual factor levels, such as a particular treatment or skeletal region. Region models included all patients who received oophorectomy, radiation, or chemotherapy, and treatment models use measurements fixed at a single region, either L4 or L5 considering skeletal heterogeneity and radiation dose heterogeneity in spine regions. Reported p-values were not adjusted for multiple testing. Unless otherwise stated, results are in terms of the mean or difference in means between groups or times, and differences are given in absolute, not relative, units. All analyses were performed using R version 2.10.1.

RESULTS

Basis material density estimates were observed to have a precision on the order of 3 mg/cm^3. Measurement precision was sufficient to distinguish the series of test solutions in the two dimensional basis material spaces (see supplemental data). In cadaver based physiological verification, the AV/TV was correlated with marrow fat measured using DECT (r=0.80) and WF-MRI (r=0.77). Table 1 summarizes demographic characteristics of all subjects participating in the clinical trial. MF was higher by (estimated change ± standard error) 0.32 ± 0.12 absolute percentage points for each additional year of age (p=0.005). Likewise, BMD was lower by 1.1 ± 0.3 mg/cm3 for each additional year of age (p<0.001).

We observed a high overall correlation (r = 0.77, 95% CI: 0.69, 0.83) between DECT and WF-MRI based MF quantification at L3, L4, and L5 for 15 subjects (Figure 1) with r = 0.80 (95% CI: 0.65, 0.89) at baseline; r = 0.68 (95% CI: 0.47, 0.81) at 6 months; r = 0.66 (95% CI: 0.44, 0.80) at 12 months. Likewise, changes in MF from 0 to 12 months were highly correlated by both imaging methods (r = 0.91, 95% CI: 0.84, 0.95).

Figure 2 shows the effect of all treatments on individual skeletal regions. At baseline, absolute percent difference in MF by DECT (Figure 2A) varied. MF in L3 and L4 were equivalent, whereas L5 MF was lower by 4% (p<0.001) and FN MF was higher by 13% (p<0.001), relative to L3 and L4. MF increased in all regions over time (p<0.001), with an estimated mean change of 7% from baseline to 12 months. The degree of change was similar among the four regions imaged (p=0.27). Using WF-MRI (Figure 2B), MF also increased in all four regions over time (p<0.002). L3–L5 MF increased by 15% from baseline to 12 months. The increase in FN MF was approximately half the increase of L3–L5 (p=0.025).

We next measured absolute percent change in MF at L4 and L5 after oopherectomy, radiation, and chemotherapy using DECT and WF-MRI (Figure 3). The majority of radiation treatment was localized to tissues overlying the L5 vertebral body. L4 MF by DECT increased by 9% after radiation, 9% after chemotherapy, and 4% after oophorectomy (p<0.032). The degree of increase in MF was larger for chemotherapy and radiation relative to oophorectomy (interaction p=0.004). Changes in L5 MF by DECT (Figure 3B) were similar to those seen in L4, although the radiation group had a larger increase in MF at L5. From 0 to 12 months, L5 MF increased by 17% with radiation, 8% with chemotherapy and 4% with oophorectomy (p<0.032). The increase in L5 MF was greater for radiation and chemotherapy, relative to oophorectomy (interaction p<0.001). Likewise, increased L4 and L5 MF from 0 to 12 months was observed by WF-MRI (Figure3C and 3D). Changes in L4

MF varied by treatment (interaction $p<0.001$), with smallest increases following oophorectomy (6%) compared to chemotherapy (24%) or radiation (19%).

Mapping of MF distribution was developed using DECT and WF-MRI. Figure 4 is a representative figure showing longitudinal changes in MF distribution in the spine associated with chemotherapy. An increase in MF throughout all marrow regions were observed at both 6 and 12 months, long after treatment completion, suggesting systemic and sustained increases in MF resulting from chemotherapy.

Figure 5 shows absolute differences in BMD in mg/cm^3 over one year by skeletal region, treatment and imaging modality. DECT-derived BMD was significantly different between skeletal regions ($p<0.01$), suggesting inherent skeletal heterogeneity (Figure 5A). At baseline, L4 was higher by 12 mg/cm^3 and L5 by 25 mg/cm^3, relative to L3. FN was lower by 47 mg/cm^3. BMD decreased in L3–L5 over time ($p<0.02$), but not FN ($p=0.24$). BMD decreased in all regions over time ($p<0.02$), but the degree of change differed among the regions (interaction $p=0.03$). The decrease in mean BMD from baseline to 12 months was 7 mg/cm^3 at L3, 14 mg/cm^3 at L4, and 13 mg/cm^3 at L5. Likewise, decreases in BMD differed by treatment. Over twelve months, L4 BMD decreased by 23 mg/cm^3 ($p=0.01$) with chemotherapy, by 10 mg/cm^3 with radiation therapy ($p=0.09$) and by 8 mg/cm^3 with oophorectomy ($p=0.24$, Figure 5B). Likewise, L5 BMD decreased by 26 mg/cm^3 ($p=0.01$) with chemotherapy, by 13 mg/cm^3 with radiation therapy ($p=0.44$) and by 3 mg/cm^3 with oophorectomy ($p=0.52$). One patient with a large BMD increase confounded the results for the radiation group at L5.

We next compared changes in L4 BMD by imaging modality and treatment (Figure5C and 5D). Relative decreases were considered for this comparison due to a different measurement scale for DXA. The median per patient relative decrease in L4 BMD was 14% by DECT, 20% by QCT, and only 5% by DXA ($p<0.002$ for all). For QCT, the median decrease in L4 BMD was 23% with radiation or chemotherapy and 11% with oophorectomy ($p=0.01$). For DECT, the corresponding reductions were 15% with radiation or chemotherapy and 9% with oophorectomy ($p=0.16$), and for DXA, 6% and 4% ($p=0.29$) with the respective cancer treatments.

Figure 6 shows correlations between L4 MF and BMD. At baseline, there was negative correlation between MF and BMD (Figure 6A, 6B). The degree of correlation varied depending on imaging modality; correlation was high when MF and BMD were measured using DECT and WF-MRI, and lower when BMD was measured using DXA. Correlations of changes of MF and BMD due to treatment effects were substantially reduced or absent (Figure 6C, 6D).

DISCUSSION

Cancer survivors' bone health is an emerging problem due to continued improvements in cancer survival rates worldwide. Appropriate predictive biomarkers are needed to identify patients at high risk of treatment induced bone injury, permitting individualized therapy to reduce bone marrow damage and long-term bone loss. We observed dramatic increases in

MF in ovariectomized mice after radiation, without an equivalent loss of either bone or hematopoietic cellularity (14). Since bone surfaces are generally quiescent following ovariectomy (34), and rapidly dividing cells are radiosensitive, we expected cytotoxic cancer treatment to have greater adverse effects on marrow than bone. We therefore designed the current study to investigate changes in MF following treatment with radiation and chemotherapy, using oophorectomy as our control.

Age related osteoporosis is associated with a strong inverse correlation between MF and BMD. In our study, the most striking observation was the lack of a strong inverse correlation between MF and BMD after cancer treatment. Instead, we observed rapid expansion of MF which did not correspond to an equivalent decrease in BMD. This phase I study stimulates the rationale for future multistep studies a) to evaluate observed phenomenon in a larger clinical trial, and b) to initiate studies to follow patients for fracture incidence. If MF and BMD are not inversely correlated following cancer therapy, BMD and MF should be measured separately. Furthermore, DECT and not DXA might be more reliable to measure BMD in cancer survivors until the potential value of MF is established in predicting fractures.

To our knowledge, ours is the first study to measure and image MF in ovarian and endometrial cancer patients using DECT and WF-MRI. Histologic verification of cadaveric bone marrow provided a foundation for clinical translation. Also, physical verification with short chain alcohols offers a possibility to use the alcohols to measure and maintain quality of prediction in clinic. Our clinical study confirms that DECT can measure changes in both MF and BMD after cancer treatment. MF increased significantly more following radiation and chemotherapy, relative to oophorectomy (interaction $p<0.001$). We therefore conclude that increased MF in cancer patients is not due to loss of ovarian function alone. Kugel et al. measured vertebral MF using magnetic resonance spectroscopy; MF increased by <1% per year between ages 30–60 in women (35). By contrast, cancer survivors in our study experienced large (9–32%) increases in MF over one year. Interestingly, regions demonstrated heterogeneity in MF at baseline. Additionally, changes in MF varied by both treatment and time. This is possibly due to differing treatment schedules for chemotherapy (several months) versus radiation (one month). In the case of radiation, the 6 to 12 month increase in MF was relatively smaller than the 0 to 6 month increase. Difference could also be due to mechanistic difference on how chemotherapy or radiation causes marrow damage and self-repair. In *in vitro* human MSCs commitment to adipogenesis are initiated very early after radiation due to increased oxidative stress and activated peroxisome proliferator-activated receptor gamma (PPAR-γ). We previously showed that chemotherapy increased marrow adipogenesis with an additional direct effect on bone (36). Whether this adipogenic process continuously increases (or stabilizes) with time with chemotherapy or radiation or chemotherapy and radiation requires further studies. Moreover, the function of marrow adipocytes is not currently known, although in some models MF may inhibit hematopoiesis, while in other studies, MF may have a protective effect on the skeleton (37).

Our study had several limitations. This is a phase I biomarker development study. Thus the sample size was relatively small and the study period was limited to one year. Subgroup analysis was limited, as numbers in each treatment group were small. Since the field of view

of second energy source was smaller than the first in DECT scanner (30 cm vs. 50 cm, respectively), one may need to be careful while deriving parameters such as MF and BMD. The measured MRI fat fraction used in this study included some bias from T1 and T2*, which could be corrected in future work with more sophisticated acquisition and reconstruction techniques (38).

Conclusions

In summary, we established the feasibility of DECT and WF-MRI to measure the impact of cancer treatment on MF and BMD. Because CT is routinely used to diagnose cancer and monitor response to therapy, DECT could characterize changes in skeletal health (MF and BMD) with little or no additional cost or radiation exposure. We suggest that MF and BMD should be considered independently, when monitoring the adverse effects of cancer therapy. Future longitudinal studies in cancer survivors are needed to determine how long increased MF persists following cancer therapy and how changes in MF associate with changes in BMD.. Most importantly, researchers need to evaluate whether measuring MF helps to predict fractures in cancer survivors, before such measurements are widely obtained in clinical practice.

Supplementary Material

Refer to Web version on PubMed Central for supplementary material.

Acknowledgement

This work was supported by the NIH (RO3 AR055333-02, 1K12-HD055887-01, NIH 8UL1TR0001114, P41 RR008079, P41 EB015894, NIH R24 DK092759, and P30 CA77398). Other grant support includes University of Minnesota seed grants (the Minnesota Medical Foundation, Academic Health Center, Grant in Aid, Breast Cancer Research). We acknowledge Matthew H Gerber for supporting recruitment.

References

1. Baxter N, Habermann E, Tepper J, Durham S, Virnig B. Risk of pelvic fractures in older women following pelvic irradiation. JAMA. 2005; 294(20):2587. [PubMed: 16304072]
2. Guise T. Bone loss and fracture risk associated with cancer therapy. The Oncologist. 2006; 11(10): 1121–1131. [PubMed: 17110632]
3. Ensrud KE, Lipschutz RC, Cauley JA, Seeley D, Nevitt MC, Scott J, Orwoll ES, Genant HK, Cummings SR. Body size and hip fracture risk in older women: a prospective study. The American journal of medicine. 1997; 103(4):274–280. [PubMed: 9382119]
4. Chen Z, Maricic M, Bassford T, Pettinger M, Ritenbaugh C, Lopez A, Barad D, Gass M, LeBoff M. Fracture risk among breast cancer survivors: Results from the Women's Health Initiative Observational Study. Archives of Internal Medicine. 2005; 165(5):552. [PubMed: 15767532]
5. Tokumaru S, Toita T, Oguchi M, Ohno T, Kato S, Niibe Y, Kazumoto T, Kodaira T, Kataoka M, Shikama N, Kenjo M, Yamauchi C, Suzuki O, Sakurai H, Teshima T, Kagami Y, Nakano T, Hiraoka M, Mitsuhashi N, Kudo S. Insufficiency fractures after pelvic radiation therapy for uterine cervical cancer: an analysis of subjects in a prospective multi-institutional trial, and cooperative study of the Japan Radiation Oncology Group (JAROG) and Japanese Radiation Oncology Study Group (JROSG). Int. J Radiat Oncol Biol Phys. 2012; 84(2):e195–e200. [PubMed: 22583605]
6. Grigsby PW, Roberts HL, Perez CA. Femoral neck fracture following groin irradiation. International Journal of Radiation Oncology* Biology* Physics. 1995; 32(1):63–67.
7. Despars G, St-Pierre Y. Bidirectional interactions between bone metabolism and hematopoiesis. Experimental hematology. 2011; 39:809–816. [PubMed: 21609752]

8. Bianco P. Minireview: The Stem Cell Next Door: Skeletal and Hematopoietic Stem Cell “Niches” in Bone. Endocrinology. 2011; 152(8):2957–2962. [PubMed: 21610157]
9. Georgiou K, Foster B, Xian C. Damage and Recovery of the Bone Marrow Microenvironment Induced by Cancer Chemotherapy-Potential Regulatory Role of Chemokine CXCL12/Receptor CXCR4 Signalling. Current Molecular Medicine. 2010; 10(5):440–453. [PubMed: 20540706]
10. Sacks E, Goris M, Glatstein E, Gilbert E, Kaplan H. Bone marrow regeneration following large field radiation. Influence of volume, age, dose, and time. Cancer. 2006; 42(3):1057–1065. [PubMed: 100197]
11. Rosen C, Ackert-Bicknell C, Rodriguez J, Pino A. Marrow fat and the bone microenvironment: developmental, functional, and pathological implications. Critical reviews in eukaryotic gene expression. 2009; 19(2):109. [PubMed: 19392647]
12. Cawthorn WP, Scheller EL, Learman BS, Parlee SD, Simon BR, Mori H, Ning X, Bree AJ, Schell B, Broome DT, Soliman SS, DelProposto JL, Lumeng CN, Mitra A, Pandit SV, Gallagher KA, Miller JD, Krishnan V, Hui SK, Bredella MA, Fazeli PK, Klibanski A, C HM, Rosen CJ, MacDougald OA. Bone Marrow Adipose Tissue Is an Endocrine Organ that Contributes to Increased Circulating Adiponectin during Caloric Restriction. Cell Metabolism. 2014 http://dx.doi.org/10.1016/j.cmet.2014.06.003.
13. Patsch JM, Li X, Baum T, Yap SP, Karampinos DC, Schwartz AV, Link TM. Bone marrow fat composition as a novel imaging biomarker in postmenopausal women with prevalent fragility fractures. J Bone Miner Res. 2013; 28(8):1721–1728. [PubMed: 23558967]
14. Hui SK, Sharkey L, Kidder LS, Zhang Y, Fairchild G, Coghill K, Xian CJ, Yee D. The Influence of Therapeutic Radiation on the Patterns of Bone Marrow in Ovary-Intact and Ovariectomized Mice. PLoS One. 2012; 7(8):e42668. [PubMed: 22880075]
15. Xian CJ, Cool JC, van Gangelen J, Foster BK, Howarth GS. Effects of Etoposide and cyclophosphamide acute chemotherapy on growth plate and metaphyseal bone in rats. Cancer Biol Ther. 2007; 6(2):170–177. [PubMed: 17218784]
16. Hui SK, Arentsen L, Wilcox A, Yee D, Ghebre RG. Spatial and temporal fracture pattern in breast and gynecologic cancer survivors. Journal of Cancer. 2014 **In Press**.
17. Goodsitt MM, Hoover P, Veldee MS, Hsueh SL. The composition of bone marrow for a dual-energy quantitative computed tomography technique: A cadaver and computer simulation study. Investigative Radiology. 1994; 29(7):695. [PubMed: 7960616]
18. Ikeda T, Sakurai K. [Influence of bone marrow fat on the determination of bone mineral content by QCT]. Nihon Igaku Hoshasen Gakkai zasshi. Nippon acta radiologica. 1994; 54(9):886–896.
19. Bolotin HH. DXA in vivo BMD methodology: An erroneous and misleading research and clinical gauge of bone mineral status, bone fragility, and bone remodelling. Bone. 2007; 41(1):138–154. [PubMed: 17481978]
20. Nickoloff E, Feldman F, Atherton J. Bone mineral assessment: new dual-energy CT approach. Radiology. 1988; 168(1):223. [PubMed: 3380964]
21. Fazeli PK, Horowitz MC, MacDougald OA, Scheller EL, Rodeheffer MS, Rosen CJ, Klibanski A. Marrow fat and bone—new perspectives. The Journal of Clinical Endocrinology & Metabolism. 2013; 98(3):935–945. [PubMed: 23393168]
22. Kalender W, Klotz E, Suess C. Vertebral bone mineral analysis: an integrated approach with CT. Radiology. 1987; 164(2):419–423. [PubMed: 3602380]
23. Sacks E, Goris M, Glatstein E, Gilbert E, Kaplan H. Bone marrow regeneration following large field radiation. Influence of volume, age, dose, and time. Cancer. 1978; 42(3):1057–1065. [PubMed: 100197]
24. Casamassima F, Ruggiero C, Caramella D, Tinacci E, Villari N, Ruggiero M. Hematopoietic bone marrow recovery after radiation therapy: MRI evaluation. Blood. 1989; 73(6):1677. [PubMed: 2713500]
25. Rubin P, Landman S, Mayer E, Keller B, Ciccio S. Bone marrow regeneration and extension after extended field irradiation in Hodgkin's disease. Cancer. 1973; 32(3):699–711. [PubMed: 4726969]
26. Bolan PJ. Magnetic Resonance Spectroscopy of the Breast: Current Status. Magnetic Resonance Imaging Clinics of North America. 2013

27. Flohr T, McCollough C, Bruder H, Petersilka M, Gruber K, Sü C, Grasruck M, Stierstorfer K, Krauss B, Raupach R. First performance evaluation of a dual-source CT (DSCT) system. European Radiology. 2006; 16(2):256–268. [PubMed: 16341833]
28. Berger MJ, Hubbell J, Seltzer S, Chang J, Coursey J, Sukumar R, Zucker D. XCOM: Photon cross sections database. NIST Standard Reference Database. 1998; 8:87–3597.
29. Johnson TR, Krauss B, Sedlmair M, Grasruck M, Bruder H, Morhard D, Fink C, Weckbach S, Lenhard M, Schmidt B. Material differentiation by dual energy CT: initial experience. European radiology. 2007; 17(6):1510–1517. [PubMed: 17151859]
30. Photon E. Proton and Neutron Interaction Data for Body Tissues. ICRU Report. 1992; 46
31. Arentsen L, Yagi M, Takahashi Y, Bolan PJ, White M, Yee D, Hui S. Validation of marrow fat assessment using noninvasive imaging with histologic examination of human bone samples. Bone. 2014
32. Bolan PJ, Arentsen L, Sueblinvong T, Zhang Y, Moeller S, Carter JS, Downs LS, Ghebre R, Yee D, Froelich J. Water–fat MRI for assessing changes in bone marrow composition due to radiation and chemotherapy in gynecologic cancer patients. Journal of Magnetic Resonance Imaging. 2013; 38:7.
33. Liang K-Y, Zeger SL. Longitudinal data analysis using generalized linear models. Biometrika. 1986; 73(1):13–22.
34. Boyce R, Franks A, Jankowsky M, Orcutt C, Piacquadio A, White J, Bevan J. Sequential histomorphometric changes in cancellous bone from ovariohysterectomized dogs. Journal of Bone and Mineral Research. 1990; 5(9):947–953. [PubMed: 2281825]
35. Kugel H, Jung C, Schulte O, Heindel W. Age-and sex-specific differences in the 1H-spectrum of vertebral bone marrow. Journal of Magnetic Resonance Imaging. 2001; 13(2):263–268. [PubMed: 11169833]
36. Fan CM, Foster BK, Hui SK, Xian CJ. Prevention of Bone Growth Defects, Increased Bone Resorption and Marrow Adiposity with Folinic Acid in Rats Receiving Long-Term Methotrexate. PLoS One. 2012; 7(10):e46915. [PubMed: 23071661]
37. Doucette CR, Rosen CJ. Seventh Meeting on Bone Quality 2012: Bone–Fat Interactions. Osteoporosis International. 2013; 24 S443-+.
38. Reeder SB, Cruite I, Hamilton G, Sirlin CB. Quantitative assessment of liver fat with magnetic resonance imaging and spectroscopy. Journal of Magnetic Resonance Imaging. 2011; 34(4):729–749. [PubMed: 21928307]

Highlights

- Dual energy CT (DECT), similar to WF-MRI, can measure change in marrow fat (MF)
- This study reveals rapid increase in MF following radiation or chemotherapy
- Lack of a strong inverse correlation between MF and BMD after cancer treatment
- MF and BMD may be monitored independently to assess skeletal damage from treatment

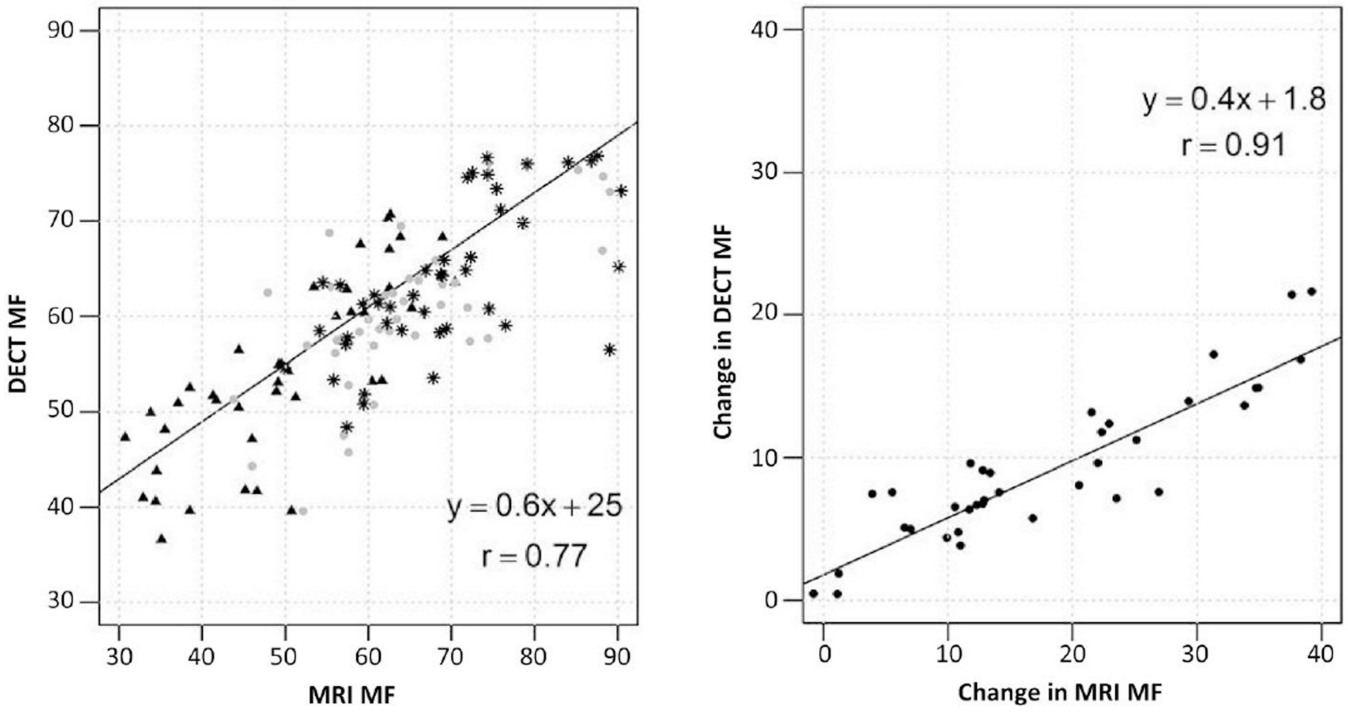

Figure 1. Correlation between DECT and WF-MRI marrow fat (MF) at L3, L4 and L5

A) A high correlation (r=0.77, 95% CI: 0.69, 0.83) in MF measurements (includes L3, L4, and L5) between the two imaging modalities was observed at baseline (triangle), 6 (circle) and 12 months (star) post treatment. B) Measurements of absolute change in MF from baseline to 12 months were highly correlated between the two imaging methods (r= 0.91, 95% CI: 0.84, 0.95)

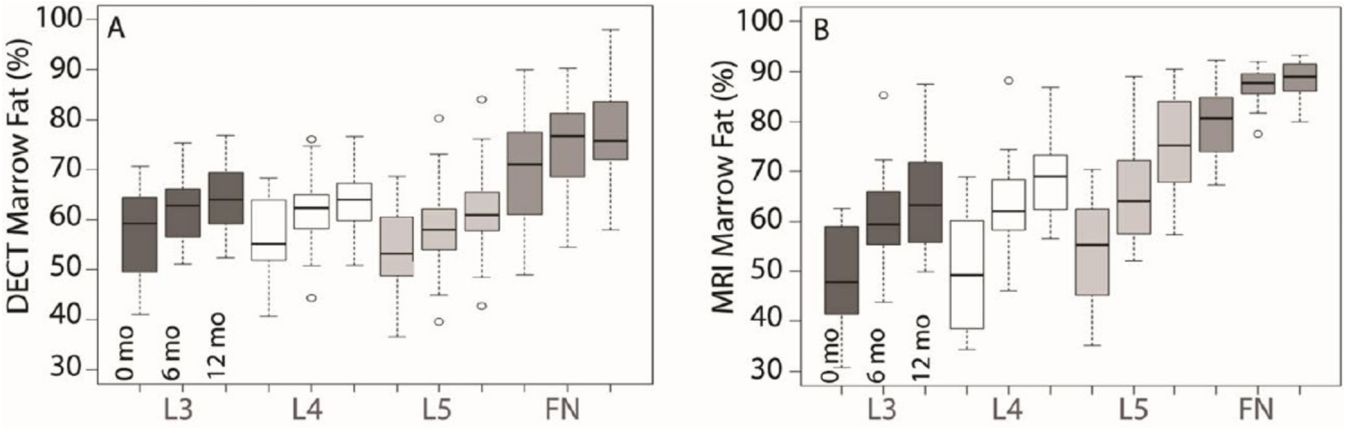

Figure 2. Region Effects of all treatments on marrow fat or MF measured by DECT (A) and MRI (B)

The region of each boxplot represents the 1st and 3rd quartile range of observations, with a black line at the median. Whisker lines are placed at the 1.5 interquartile range of the lower and upper quartile and outliers are noted with open circles. **A. DECT:** Regions differed in mean MF at baseline. L3 and L4 were equivalent, and L5 was lower by 4% ($p<0.001$) and FN higher by 13% ($p<0.001$) relative to L3 and L4. MF increased over time at all sites measured ($p<0.001$), with an estimated mean change of 7% from baseline to 12 months for all regions. The degree of change in MF was similar among the four regions ($p=0.27$). **B. MRI:** Regions differed in mean MF at baseline. L3 and L4 were equivalent, L5 was higher by 5%, and FN was higher by 32% ($p<0.001$). MF increased over time at all sites measured ($p<0.002$), with an estimated mean change of 15% from baseline to 12 months for L3–L5. In contrast to DECT, the increase in FN MF was approximately half the increase of L3–L5 ($p=0.025$).

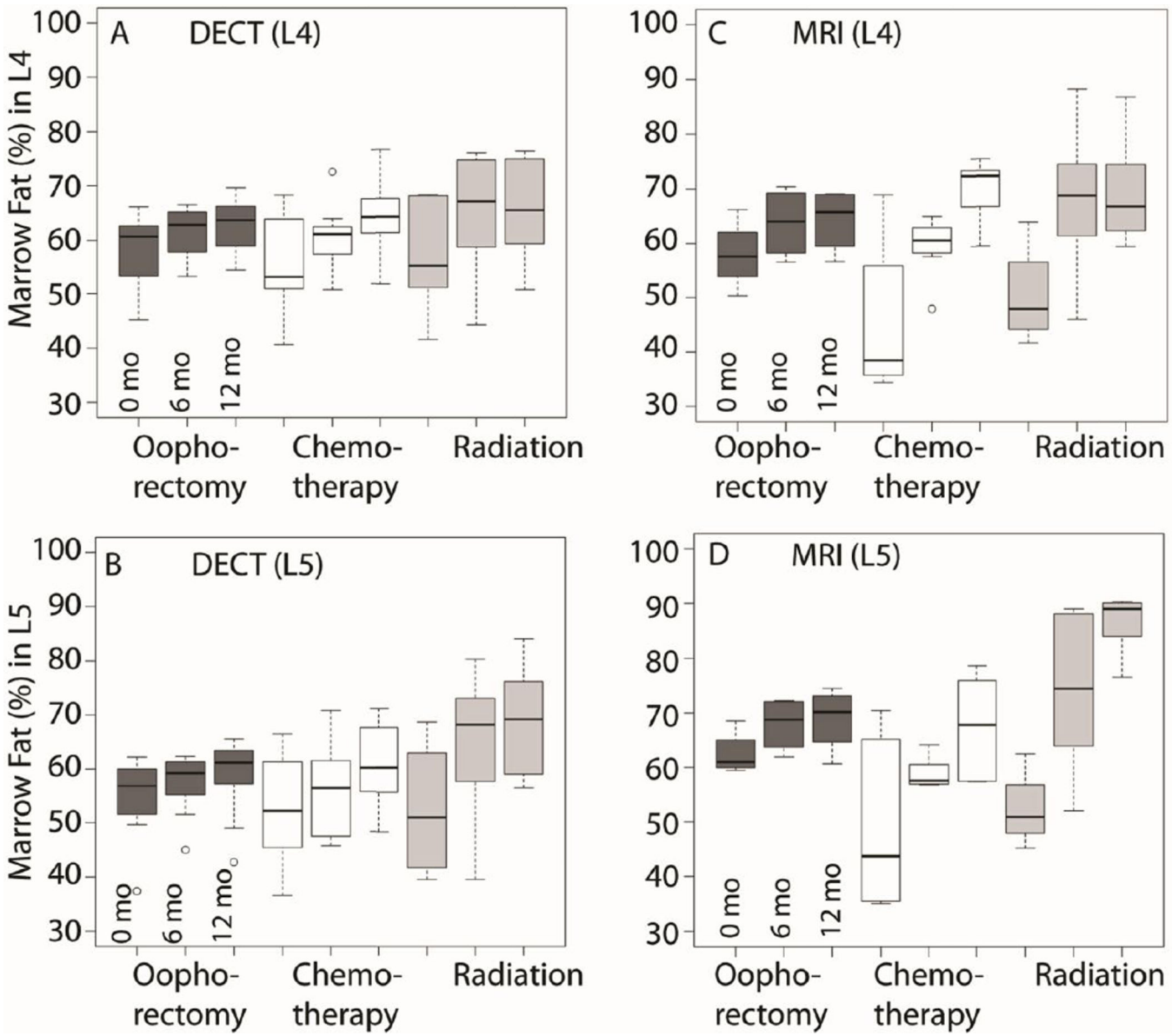

Figure 3. Absolute Percent Change in L4 and L5 Marrow Fat by Treatment

A & B: Based on dual energy computed tomography (DECT) imaging in 15 subjects from 0 to 12 months, L4 MF increased by 9% after radiation, 9% after chemotherapy, and 4% after oophorectomy ($p<0.032$). The increase in MF was larger for chemotherapy and radiation relative to oophorectomy (interaction $p=0.004$). From 0 to 12 months, L5 MF increased by 17% with radiation, 8% with chemotherapy and 4% with oophorectomy ($p<0.032$). The change varied based on treatment (time × treatment interaction $p<0.001$). C & D: By water-fat MRI imaging, L4 and L5 MF increased from 0 to 12 months. The change varied based on treatment (time × treatment interaction $p<0.001$). L4 MF increased by 19% after radiation, by 24% after chemotherapy, and by 6% after oophorectomy. Likewise, L5 MF by WF-MRI increased from 0 to 12 months. L5 MF increased by 32% after radiation, by 18% after chemotherapy, and by 6% after oophorectomy.

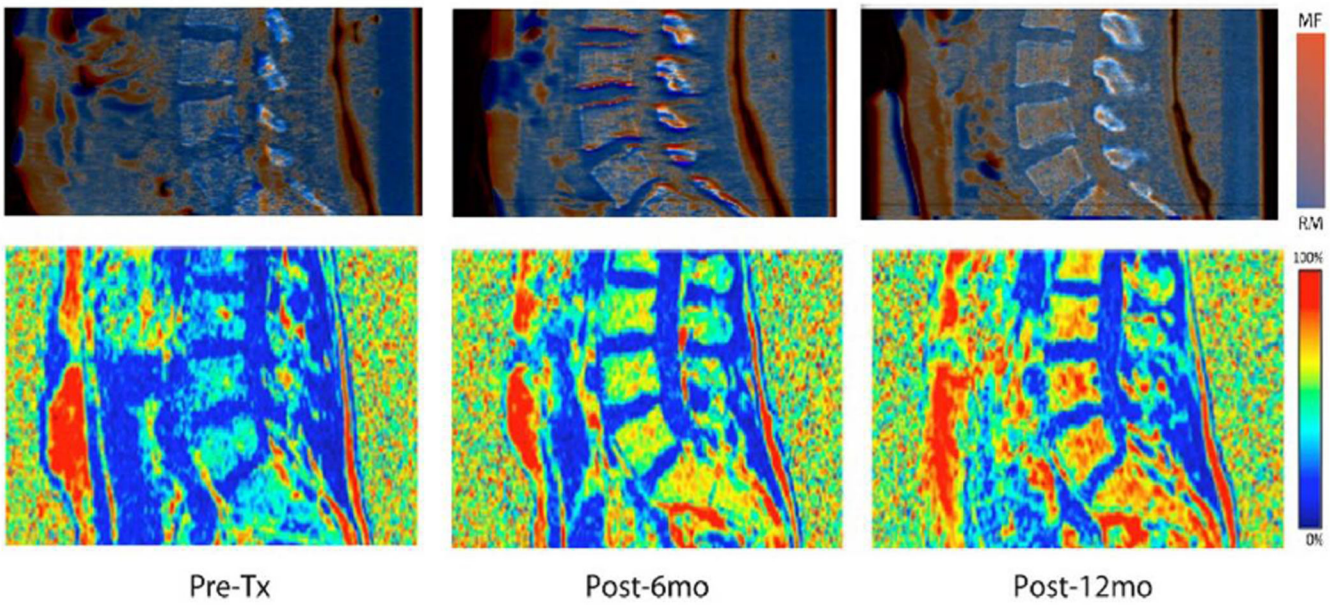

Figure 4. Marrow fat mapping of a representative patient using DECT and water-fat MRI

Spine marrow fat mapping: Longitudinal changes in marrow fat distribution in spine due to chemotherapy for a representative subject at a) baseline, B) 6 months and C) 12 months after treatment using DECT (top figure) and water-fat MRI (bottom figure). Changes in MF were visible within 6 months of treatment, and continued to increase at 12 months.

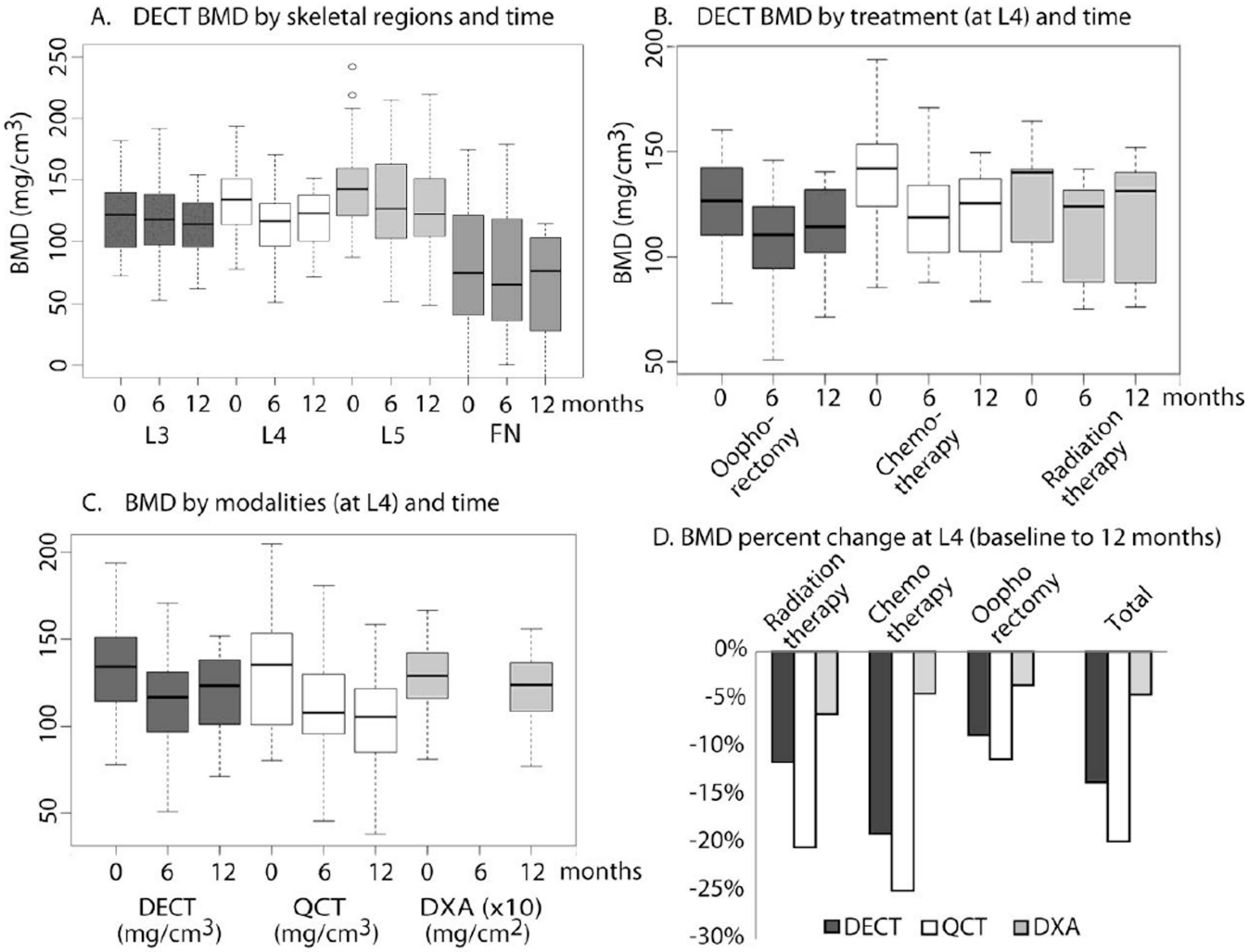

Figure 5. (Sensitivity): BMD changes measured by different techniques

A. DECT BMD by skeletal regions and time: Regions differed in mean BMD at baseline ($p<0.001$); L4 was higher by 12 mg/cm^3 and L5 by 25 mg/cm^3 relative to L3. BMD in all regions decreased over time ($p<0.02$), and change varied by region (time × region interaction $p=0.03$).The 12 month decrease in BMD was 7 mg/cm^3 at L3, 14 mg/cm^3 at L4, and 13 mg/cm^3 at L5. FN was lower by 47 mg/cm^3. **B. DECT BMD by treatment (at L4) and time:** Mean BMD measured by DECT at L4 did not vary at baseline based on treatment ($p=0.42$). Chemotherapy decreased BMD by 23 mg/cm^3 ($p=0.01$) from 0 to 12 months. Radiation decreased BMD by 10 mg/cm^3 ($p=0.09$) from 0 to 12 months, and was lowest at 6 months. Oophorectomy decreased BMD by 8 mg/cm^3 from 0 to 12 months ($p=0.24$) and was lowest at 6 months. A similar pattern was seen at L5. Mean BMD decrease from baseline to 12 months was 3 mg/cm^3 for oophorectomy ($p=0.52$), 26 mg/cm^3 for chemotherapy ($p=0.01$), and 13 mg/cm^3 for radiation ($p=0.44$). **C &D. BMD by modalities (at L4) and time:** The median per patient BMD percent decrease was 14% for DECT, 20% for QCT, and 5% for DXA ($p<0.002$ for all). The degree of decrease was larger in patients treated with chemotherapy or radiation compared to oophorectomy, and was statistically significant for QCT ($p=0.01$), but not DECT ($p=0.16$) or DXA ($p=0.29$). Note: left figure

(6c) shows absolute measurement and right figure (6 d) shows relative change in BMD between baseline and 12 months.

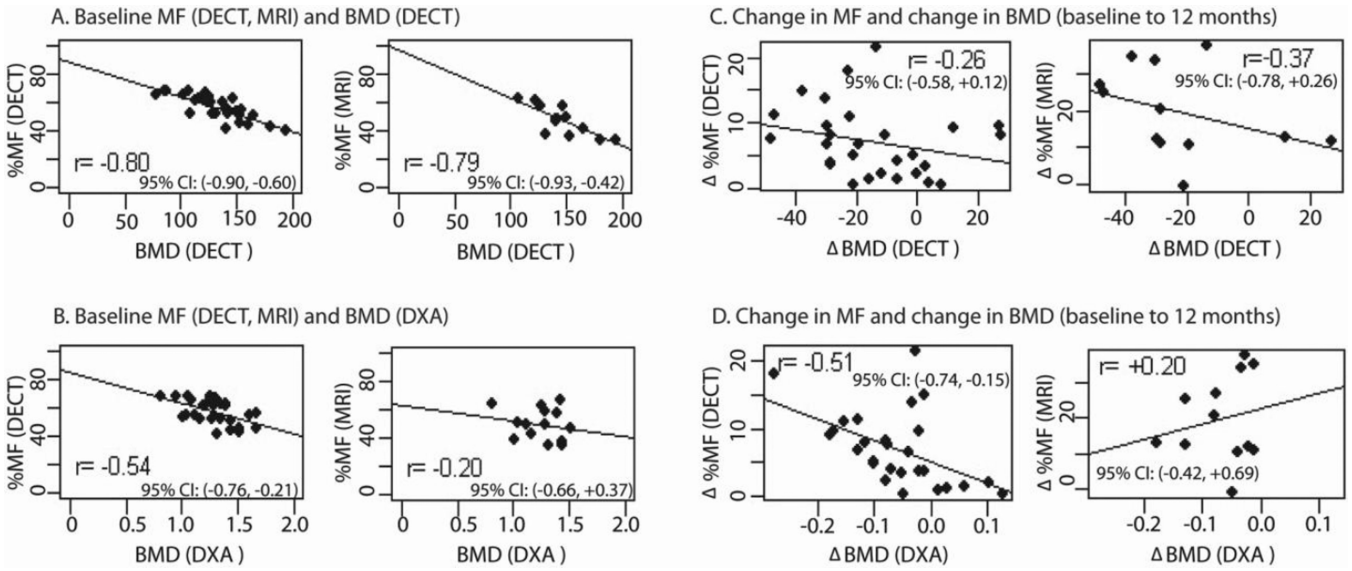

Figure 6.

Correlation of MF and BMD at L4 from different modalities measuring the same patient. The panel on the left shows absolute measurements at baseline. The panel on the right shows changes from baseline to 12 months.

Table 1

Demographic Characteristics of Subjects

Data are summarized using the mean ± standard deviation. Chemotherapy was the principal treatment modality for ovarian cancer, radiation therapy was primarily used to treat endometrial cancer, and oophorectomy was performed in early stage ovarian and endometrial cancer patients who did not require subsequent radiation or chemotherapy.

	Treatment modalities (cancer type)		
Variable	**Chemotherapy**	**Radiation Therapy**	**Oophorectomy**
Sample Size	13	6	12
Age, years	55 ± 17	52 ± 7	53 ± 6
Body Mass Index, kg/m^2	27 ± 5	32 ± 6	35 ± 6
DXA % Fat at baseline	42 ± 8	46 ± 7	48 ± 6
DXA % Fat at 12 months	43 ± 7	44 ± 10	49 ± 5